

# Mapping land cover based on time series synthetic aperture radar (SAR) data in Klaten, Indonesia

**Vidya Nahdhiyatul Fikriyah**

Faculty of Geography, Universitas Muhammadiyah Surakarta, Surakarta, Indonesia

E-mail: [vidya.n.fikriyah@ums.ac.id](mailto:vidya.n.fikriyah@ums.ac.id)

***Abstract.** Information on the existing land cover is important for land management and planning because it can represent the intensity, location, and pattern of human activities. However, mapping land cover in tropical regions is not easy when using optical remote sensing due to the scarcity of cloud-free images. Therefore, the objective of this study is to map the land cover in Klaten Regency using a time-series Sentinel-1 data. Sentinel-1 data is one of remote sensing images with Synthetic Aperture Radar (SAR) system which is well known by its capability of cloud penetration and all-weather observation. A time-series Sentinel-1 data of both polarisations, VV and VH were automatically classified using an unsupervised classification technique, ISODATA. The results show that the land cover classifications obtained overall accuracies of 79.26% and 73.79% for VV and VH respectively. It is also found that Klaten is still dominated by the vegetated land (agriculture and non-agricultural land). These results suggest the opportunity of mapping land cover using SAR multi temporal data.*

***Keywords:** Land cover; Synthetic Aperture Radar; Time series; Sentinel-1; Klaten*

## 1. Introduction

The need for the existing land cover data cannot be separated from its crucial role to support strategic regional planning. In addition to the field survey method, remote sensing technology plays a role for extracting and monitoring land cover since remote sensing offers variation on spectral, temporal, and spatial resolution (Mohajane et al., 2018; Sari and Kushardono, 2014; Zhang et al., 2013). Remote sensing with optical sensor has been mostly used for this purpose. However, image quality and mapping accuracy using optical sensors depend on atmospheric conditions and this is a challenge in the observation of tropical areas that are known to have a lot of cloud cover (Trisakti and Hamzah, 2013).

In regards to dealing with cloud problem, there is Synthetic Aperture Radar (SAR) which is a remote sensing of active system, which has an advantage of the recording system that is not affected by weather conditions. SAR satellites use microwaves to detect objects, in which the object's condition will be detected from the amount of energy reflected (backscatter). Characteristics of SAR varies in the aspects of wavelength, angle of incidence, and polarization which will affect the level of sensitivity in identifying objects (Lee et al., 2009). Regarding SAR applications for land cover, several studies have attempted to use SAR data to map land cover, for example using data of RADARSAT (Ban and Wu, 2005), ERS-1/2 (Engdahl & Hyypä, 2003), and one acquisition time of Sentinel-1 (Abdikan et al., 2016).

Among other SAR data, Sentinel-1 data has 20 m of spatial resolution and 12 days revisit time (6 days for several regions if Sentinel-1A and 1B included together). This data offers two type of polarisations, single and dual polarisations, and can also be accessed freely at no charge which is an advantage compared to previous satellite imagery with SAR system, such as ERS-1, ERS-2, and ENVISAT (European Space Agency (ESA), 2013).

Previous studies have shown the ability of remote sensing technology for extracting land cover data. However, less is known about the ability of SAR sensor especially Sentinel-1 to map the land cover. Therefore, this study aim to map land cover using time series Sentinel-1 imagery. Processing using time series data enable the observation of backscatter changes of each land cover. Classification will be based on unsupervised method, which determine land cover class according to spectral characteristics. The study area is Klaten Regency, which is one of the “national rice bowl” region in Indonesia. The results of this study can be useful as an inventory of the latest land cover data for regional planning purposes, in particular related to food security.

## 2. Methodology

### 2.1 Study Area

The study is located in Klaten Regency of Central Java Province which lies between 7°32'19" to 7°48'33" South Latitude and 110°26'14" to 110°47'51" East Longitude (Figure 1). Regarding the topographic condition, most of the area in Klaten is flat (Priyono et al., 2016). Klaten is well known as one of the national ‘rice bowl’ with a total harvested area of 70,603 hectares and a total production of 406,270 tons in 2016 (BPS (Central Bureau of Statistic), 2017). With the high production, this makes agriculture becomes a primary sector in Klaten (Priyono et al., 2016).

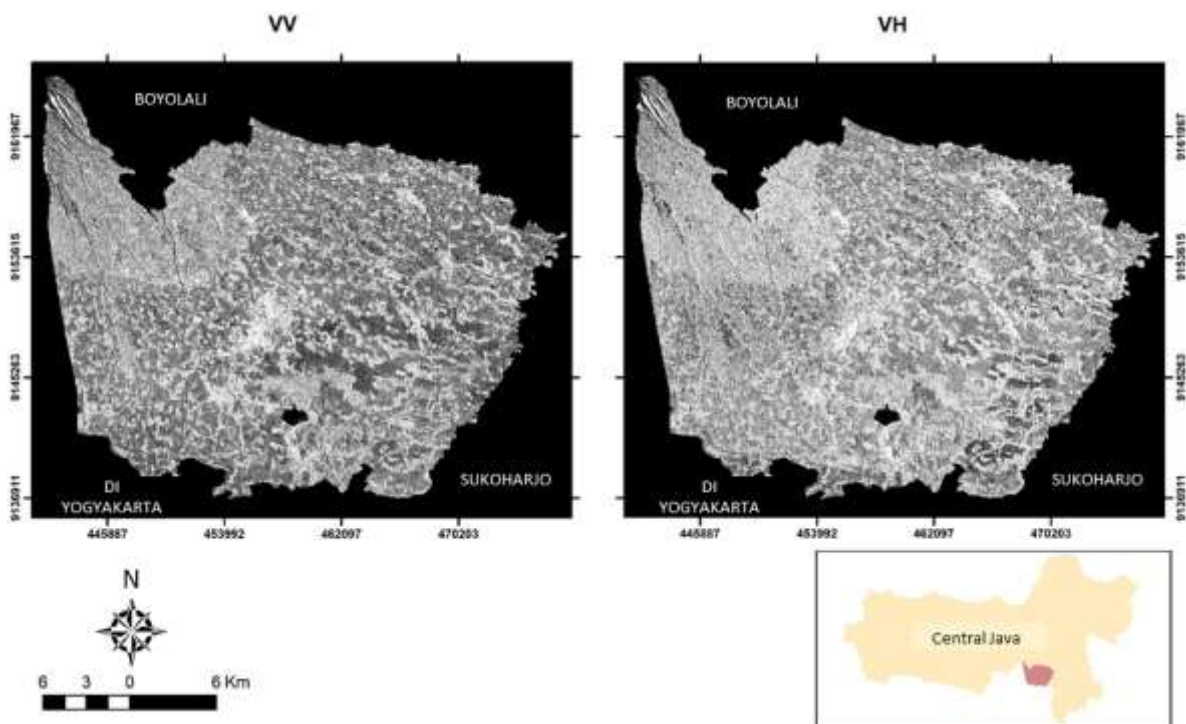


**Figure 1.** Sentinel-1A recorded in Klaten area, July 1, 2018

### 2.2 Data Processing

Sentinel-1 was developed by European Space Agency (ESA) and launched in April 2014 under Copernicus Project. In this study, a time-series of Sentinel-1A data was used to extract the temporal backscatter of land cover/land use classes. Sentinel-1A and 1B have different orbital directions in their recording (descending and ascending pass), therefore this study only used Sentinel-1A data for data consistency. Level 1 Ground Range Detected (GRD) of Sentinel-1A with dual polarisations (VV and VH) images and mode of Interferometric Wide Swath (IW) were downloaded from the ESA catalogue data portal <https://scihub.copernicus.eu/dhus/#/home>. Date of acquisition is from 15 March 2018 to 1

July 2018. Ground Range Detected product is multi-looked and projected data and Interferometric Wide Swath mode is the operational mode for land observation and monitoring (ESA, 2013).

Sentinel-1 supports acquisition in single (VV or HH) and dual polarisation (VV+VH and HH+HV). Configuration of polarisation refers to how SAR signal is transmitted and received, vertically or horizontally. This study used dual polarisation mode (VV+VH) considering the data availability in the study area, and to enable the performance comparison between VV and VH polarisation.

All of Sentinel-1A data were radiometrically calibrated, multi-temporal speckle filtered (Refined Lee) (Argenti et al., 2013), and terrain corrected using tools in Sentinel Toolboxes (SNAP) developed by ESA. For the terrain correction, data of 90 m Shuttle Radar Topography Mission (SRTM) were used. Finally, images were then clipped using Klaten boundaries from Global Administrative Area (GADM) data and stacked according to their polarisations (VV and VH). The detail specification of images used in this study is given in Table 1.

**Table 1.** Sentinel-1 specification used in the study

Parameter	Description
Satellite	Sentinel-1A
Orbit/height/inclination	ascending/ 693 km/98,18°
Wavelength	C (3,75 – 7,5 cm)/ 5,405 GHz
Spatial/ temporal resolution	12 days/ 20 m
Polarisations	Dual polarisations (VV and VH)
Incidence angle	30°-46°
Mode	Interferometric Wide swath (IW)
Level	Level-1 Ground Range Detected (GRD)
Acquisition dates	10 scenes from March to July 2018 (15/3/18; 27/3/18; 8/4/18; 20/4/18; 2/5/18; 14/5/18; 26/6/18; 7/6/18; 19/6/18; 1/7/18)

Source: European Space Agency (2013)

The first stage of method was data collection, consisting of Sentinel-1A imagery and administrative boundary of Klaten Regency from the Database of Global Administrative Areas (GADM) by accessing <https://gadm.org>. To enable the accuracy test, the ground truth data was obtained from visual interpretation of high-resolution imagery provided through Google Earth.

The next step was the image pre-processing stage. Image pre-processing is done automatically in the SNAP (Sentinel Application Toolbox) toolbox 6.0, which is an open source software (<http://step.esa.int/main/download/>) and developed by ESA for image processing. There are several steps in pre-processing Sentinel-1A, namely (1) the application of the 'apply orbit file' feature to update satellite position information, (2) calibration of the radiometric value to convert the intensity value in the raw data image to the sigma nought value ( $\sigma^\circ$ ), then the actual backscatter value of the object can be obtained, (3) the separation of image data into two stacks for VV and VH polarization, then (4) filtering to eliminate speckle interference in each polarization with the Multi-temporal Refined Lee technique, then the last process, (5) terrain correction using the Range Doppler method to reduce distortion caused by topographic aspects and to register images to the 1984 WGS Geographic projection system. Terrain correction uses Digital Elevation Model (DEM) data reference from the Shuttle Radar Topography Mission (SRTM) with 90 m resolution.

Another process was extracting backscatter values for each land cover class. Digital Number (DN) in the image represent the intensity of the radar signal. To plot backscatter values on a multi-time basis, the previous DN value was converted to decibels (dB) according to the following formula (Veci, 2015).

$$\text{backscatter (dB)} = 10 * \log_{10} (\text{DN}) \dots\dots\dots (1)$$

The algorithm used to classify images is Iterative Self-Organizing Data Analysis (ISODATA). ISODATA is an unsupervised classification technique that classifies object spectral values

automatically, therefore it does not require training area information (Khoi and Munthali, 2012). The classification would be based on the spectral variation in the images. In this study, the number of clusters was determined to be five to ten, and the iteration was carried out ten times.

From the results of the classification, class evaluations and labeling were then conducted based on visual observation. The final stage was evaluating the results of classification by comparing classification results with ground truth data. In total, 40 polygons from high spatial resolution images in Google Earth (recording time range from March to May 2018) were obtained. The accuracy value was then calculated in the overall accuracy value and Kappa coefficient. In summary, the research method is shown in Figure 2.

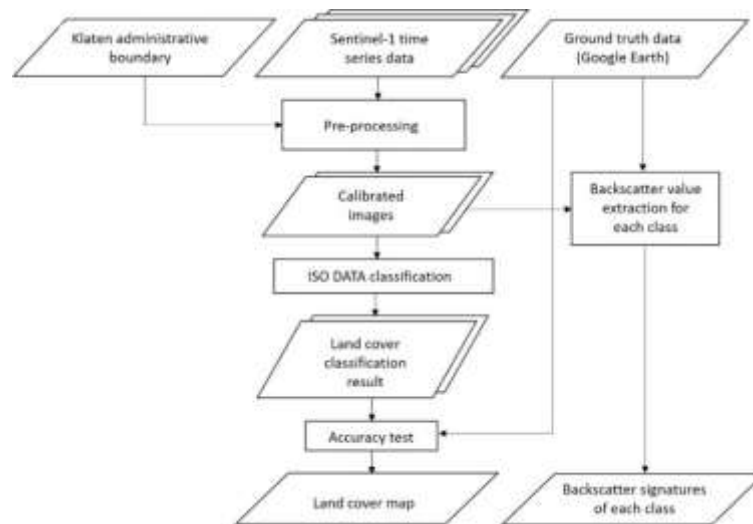


**Figure 2.** Flowchart for land cover mapping

### 3. Result and Discussion

#### 3.1 Observation of Sentinel-1 Time Series Data

For the visual analysis, three images were selected to represent the difference of recording time (27 March 2018, 7 June 2018, and 1 July 2018). We can see difference in brightness from the three Sentinel-1A recording times as shown in Figure 3. Variations in brightness in the figures indicate temporal variation in backscatter values.

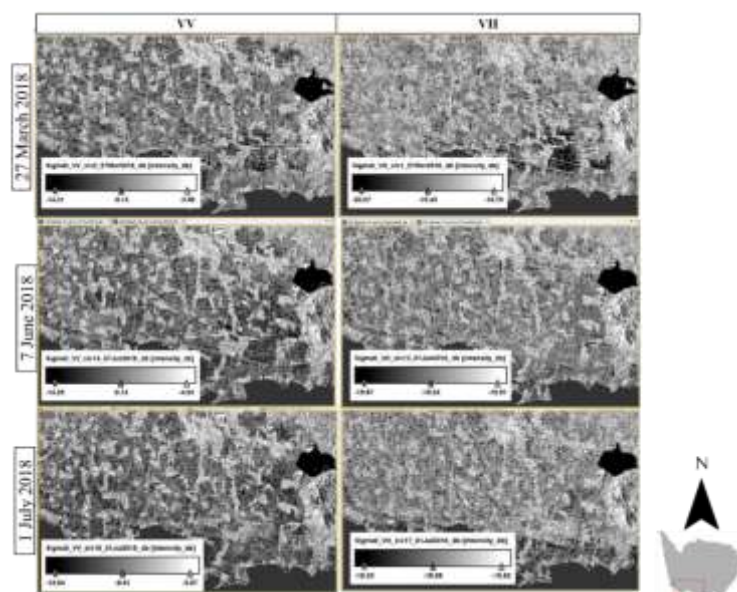


**Figure 3.** Difference in brightness recorded in the Sentinel-1A image

Visual observation was also conducted to identify land covers. Class of land cover can be seen from the difference in brightness and colour on the RGB composite image from a combination of three time-recorded images (Figure 4). As shown in Figure 4, colour contrast is more visible on the image with VV polarisation than VH. Despite the variation in colour, there are similarities characteristics observed in both polarisations. Water body was seen black in either VV and VH polarisation. This condition indicates a low backscatter signal. This condition can be explained by the specular effect, which happens due to low energy of backscatter received by the SAR sensor when SAR waves meeting objects with smooth and flat surfaces (Kasischke et al., 1996). The built-up area looks bright white, meaning that built-up object always gives a high backscatter signal all the time. This phenomenon may correlate to the SAR signal that experiences a double bounce, thereby strengthening the backscatter that returns to the satellite sensor (Tso & Mather, 2009).

For class of vegetation which is not belong to agricultural land (such as forest and shrubs), the object was seen very bright but with spot. Whereas the object of agricultural land varied in colors from to field to field. This variation means the difference in land conditions at the three time of recording. Distinct characteristic in land conditions are as a result of diversity in the timing of agricultural land management and differences in phases of plant growth that affect amount of backscatter captured by SAR sensor (Koppe et al., 2013).

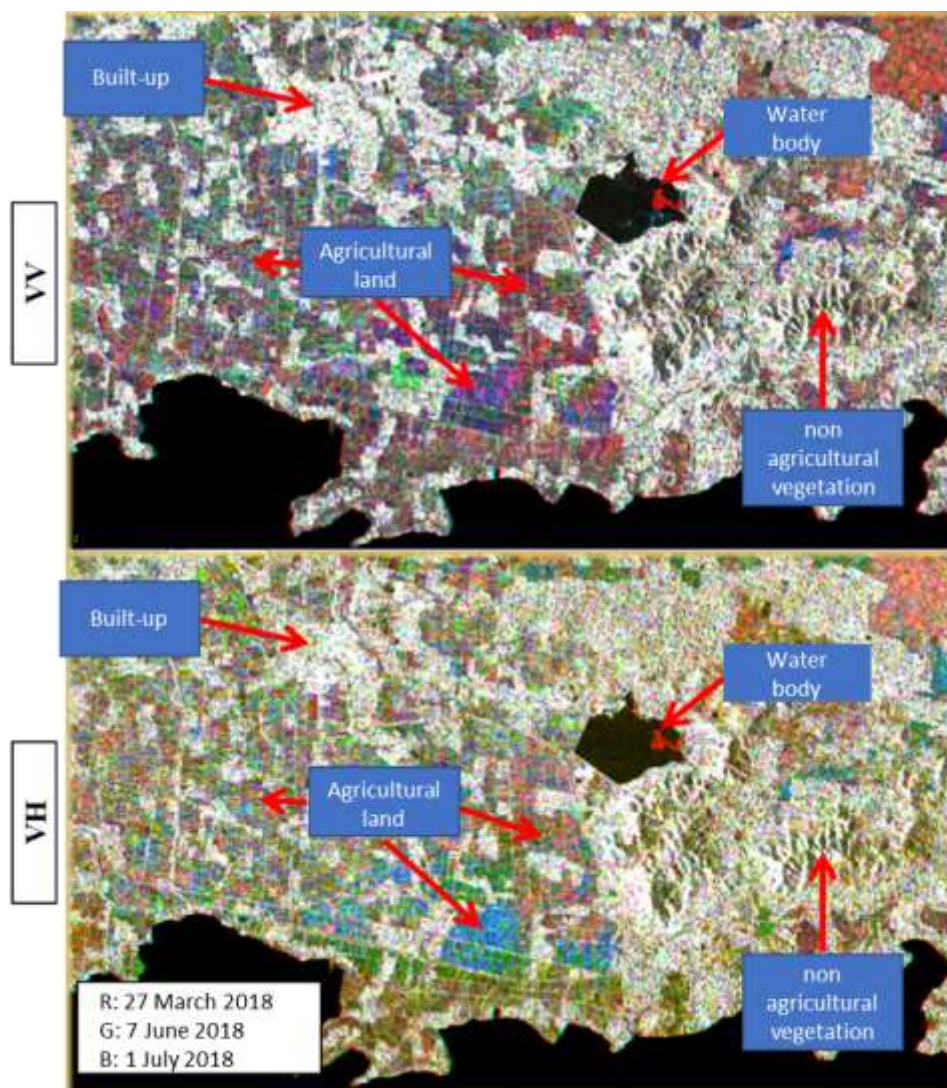


**Figure 4.** Land cover shown on the composite Sentinel-1A. RGB: 27 March, 7 June, and 1 July 2018

### 3.2 Backscatter Patterns of Land Cover

The temporal backscatter signatures of all land cover classes are presented in Figure 5. To show the backscatter variation of each land cover class temporally, average backscatter (dB) value was extracted from all ground truth polygons at each time of image recording. According to Figure 5, it can be seen that the highest backscatter value in VV and VH polarisations came from built-up class, while the lowest backscatter value were from water body object.

Moreover, other two classes, the vegetation from agricultural and non-agricultural land, provided different patterns temporally. The non-agricultural vegetation gave a higher backscatter value and a more constant pattern throughout the time of image recording, in comparison to vegetation in the agricultural land. Backscatter of agricultural land had a more varied value especially when viewed with VH polarisation (Figure 5b). Since rice is the dominant crop type in Klaten, this backscattering changes may be associated with the growth phases (vegetative, reproductive, and ripening) (Lam-Dao et al., 2009). Low backscattering values can be seen at the beginning of rice planting because of irrigation which makes the key characteristic to the detection of rice field using SAR (Bouvet and Le Toan, 2011).

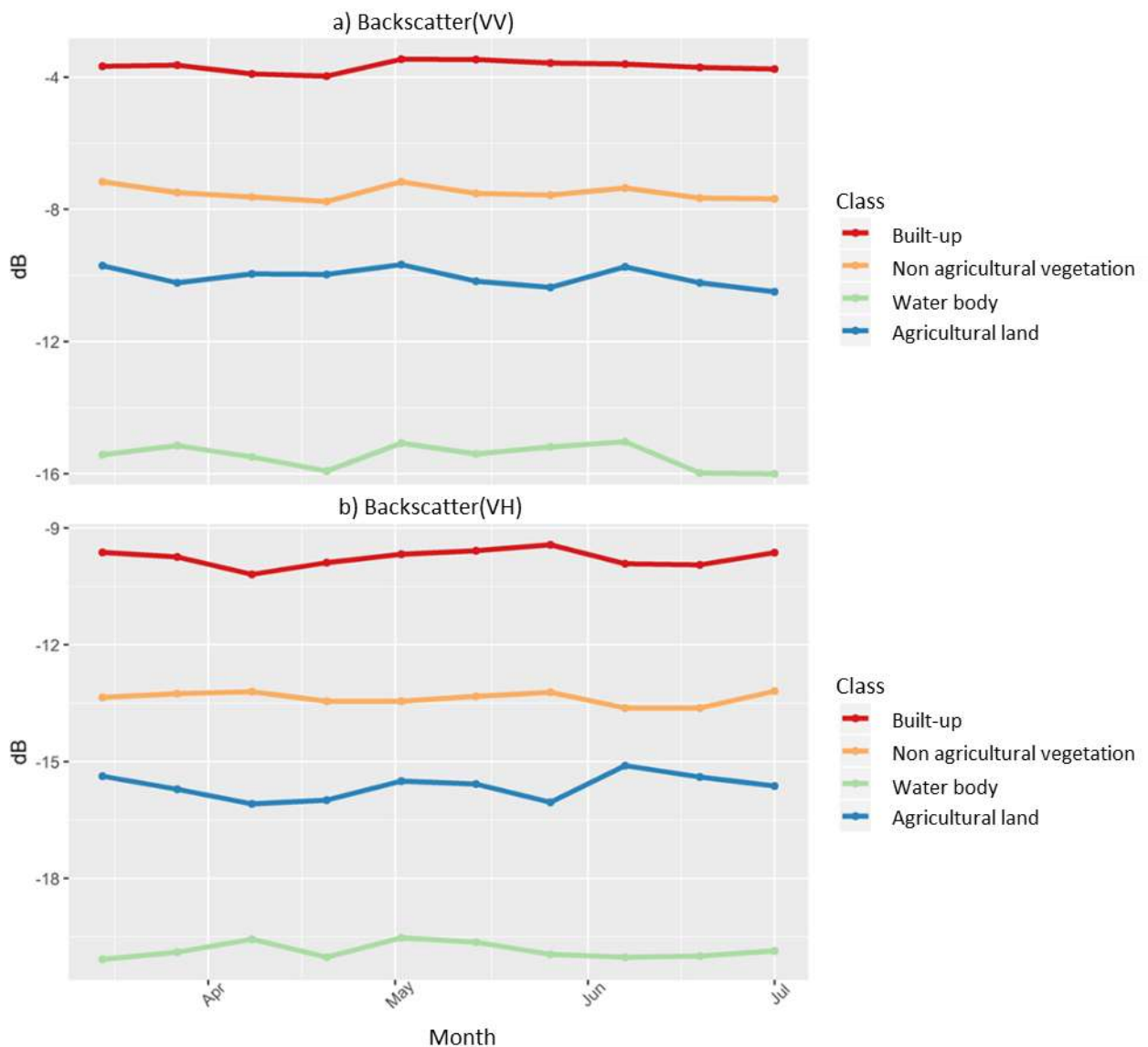


**Figure 5.** Temporal backscatter signature for each land cover class in the VV (a) and VH (b) polarisation

### 3.3 Land Cover Classification of Klaten

Figure 6 presents the results of the classification of VV and VH polarisation, while Table 2 and Table 3 show the results of accuracy assessment for VV and VH respectively. Based on the results of the classification, it is obtained that the VV polarisation gave an accuracy of 79,26% and a Kappa coefficient of 0,7. Accuracy value of VV is better when compared to the results of the classification using VH polarisation (a total accuracy of 73,79% and a Kappa coefficient of 0,63). This finding, which shows that a higher accuracy obtained by VV than VH is in line with the results obtained by Abdikan et al. (2016) who used Sentinel-1A (with only one time recording) to map land cover/use. In comparison to Balzter et al. (2015) who reached almost 70% overall accuracy with Sentinel-1, and Longép   et al. (2011) who gained 72,2% with ALOS PALSAR, this study achieved a good accuracy. Furthermore, according to Richards and Jia (2006) the resulted Kappa coefficient values from both polarisations are classified as good accuracy values.

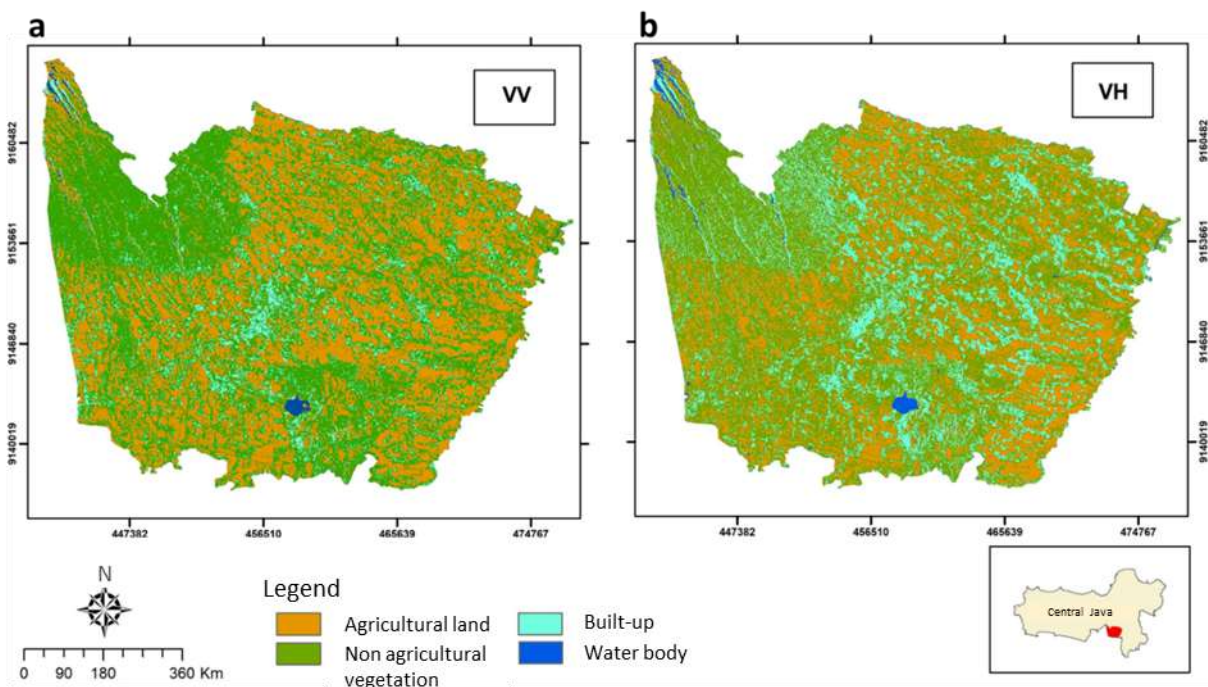


**Figure 6.** Results of land cover classification from VV polarisation (left) and VH (right)

**Table 2.** The accuracy value of the classification with VV polarisation

Class	Ground truth (pixel)				Producer accuracy (%)	User accuracy (%)
	Water body	Agricultural land	Non-agricultural vegetation	Built-up		
Water body	22	0	0	0	68,75	100
Agricultural land	9	146	5	0	75,65	91,25
Non-agricultural vegetation	0	47	134	32	88,18	62,91
Built-up	1	0	13	107	76,98	88,43
Overall accuracy (%)	79,26					
Kappa coefficient	0,7					

**Table 3.** The accuracy value of the classification with VH polarisation

Class	Ground truth (pixel)				Producer accuracy (%)	User accuracy (%)
	Water body	Agricultural land	Non-agricultural vegetation	Built-up		
Water body	26	0	0	0	83,87	100
Agricultural land	4	111	4	0	57,51	93,28
Non-agricultural vegetation	1	82	106	2	69,74	55,5
Built-up	0	0	42	137	98,56	76,54
Overall accuracy (%)	73,79					
Kappa coefficient	0,63					

Total area of each land cover class in Klaten is presented in Table 4. Areas were calculated based on the classification with a highest accuracy (VV polarisation). From the calculation of land cover area (Table 4), it can be seen that the widest land cover class belongs to the non-agricultural vegetation (34,461 Ha). This class is mostly distributed in the northwest of Klaten (Figure 6). The second largest land cover was agricultural land, with a total area up to 28.106 Ha (or 40,62% of the total Klaten area) which is spread throughout the whole Klaten area. These results indicate that land with vegetation cover still dominates Klaten Regency.

**Table 4.** Area of land cover

Class	Area (Ha)	%
Water body	463	0.67
Built-up	6.161	8.90
Agricultural land	28.106	40.62
Non-agricultural vegetation	34.461	49.81
Total	69.191	

#### 4. Conclusion

In this study, the time series Sentinel-1 data has been utilized for the classification and mapping of land cover in Klaten Regency. The results show that there are difference in backscatter pattern temporally for each land cover class which allows the classification. Utilization of time series Sentinel-1 images combined with ISO DATA classification algorithm has given results with different overall accuracy depending on the polarisation used. Classification with VV polarisation produced overall accuracy of 79.26% with Kappa coefficient of 0.7, while classification with VH polarisation gave an accuracy of 73.79% with Kappa coefficient of 0.63. Based on the results, it can be concluded that vegetated land, for both agriculture and non-agricultural land, became the dominant land cover in Klaten Regency. Therefore, the present study have shown that a multi-time Sentinel-1 image is very potential to be used for mapping land cover in tropical areas. For further studies, this image needs to be applied for monitoring, especially the agricultural land as an effort to support food security at the national level.

#### References

- Abdikan, S., Sanli, F.B., Ustuner, M., Calò, F. (2016) Land cover mapping using sentinel-1 SAR data. *Int. Arch. Photogramm. Remote Sens. Spat. Inf. Sci. - ISPRS Arch.* 41, 757–761. doi:10.5194/isprsarchives-XLI-B7-757-2016

- Argenti, F., Lapini, A., Bianchi, T., Alparone, L. (2013) A Tutorial on Speckle Reduction in Synthetic Aperture Radar Images A Tutorial on Speckle Reduction in Synthetic Aperture Radar Images. *IEEE Geosci. Remote Sens. Mag.*, 1, 6–35. doi:10.1109/MGRS.2013.2277512
- Balzter, H., Cole, B., Thiel, C., Schmillius, C. (2015) Mapping CORINE land cover from Sentinel-1A SAR and SRTM digital elevation model data using random forests. *Remote Sens.*, 7, 14876–14898. doi:10.3390/rs71114876
- Ban, Y., Wu, Q. (2005) RADARSAT SAR data for landuse/land-cover classification in the rural-urban fringe of the Greater Toronto Area, in: *Proceedings 2005 - The 8th AGILE International Conference on Geographic Information Science*, AGILE 2005.
- Bouvet, A., Le Toan, T. (2011) Use of ENVISAT/ASAR wide-swath data for timely rice fields mapping in the Mekong River Delta. *Remote Sens. Environ.*, 115, 1090–1101. doi:10.1016/j.rse.2010.12.014
- BPS (2017) *Statistik Padi Tahun 2017*. BPS (Central Bureau of Statistics) Klaten, Klaten.
- Engdahl, M.E., Hyypä, J.M. (2003) Land-cover classification using multitemporal ERS-1/2 InSAR data. *IEEE Trans. Geosci. Remote Sens.*, 41, 1620–1628. doi:10.1109/TGRS.2003.813271
- European Space Agency (ESA) (2013) *ESA Sentinel 1 handbook*, European Space Agency technical note. doi:10.1017/CBO9781107415324.004
- Kasischke, E.S., Melack, J.M., Dobson, M.C. (1996) The Use of Imaging Radars for Ecological Applications - A Review. *Remote SENS. ENVIRON. Sci. Inc.*, 59, 141–156.
- Khoi, D.D., Munthali, K.G. (2012) *Multispectral Classification of Remote Sensing Data for Geospatial Analysis*, in: *Progress in Geospatial Analysis*. Springer Japan, Tokyo, pp. 13–28. doi:10.1007/978-4-431-54000-7\_2
- Koppe, W., Gnyp, M.L., Hütt, C., Yao, Y., Miao, Y., Chen, X., Bareth, G. (2013) Rice monitoring with multi-temporal and dual-polarimetric TerraSAR-X data. *Int. J. Appl. Earth Obs. Geoinf.*, 21, 568–576. doi:10.1016/j.jag.2012.07.016
- Lam-Dao, N., Le Toan, T., Apan, A., Bouvet, A., Young, F., Le-Van, T. (2009) Effects of changing rice cultural practices on C-band synthetic aperture radar backscatter using Envisat advanced synthetic aperture radar data in the Mekong River Delta. *J. Appl. Remote Sens.*, 3, 033563. doi:10.1117/1.3271046
- Lee, J.-S., Pottier, E., Thompson, B.J. (2009) *Polarimetric radar imaging : from basics to applications*, 1st ed. CRC Press, Baton Rouge.
- Longépé, N., Rakwatin, P., Isoguchi, O., Shimada, M., Uryu, Y., Yulianto, K. (2011) Assessment of ALOS PALSAR 50 m orthorectified FBD data for regional land cover classification by support vector machines. *IEEE Trans. Geosci. Remote Sens.*, 49, 2135–2150. doi:10.1109/TGRS.2010.2102041
- Mohajane, M., Essahlaoui, A., Oudija, F., Hafyani, M. El, Hmairi, A. El, Ouali, A. El, Randazzo, G., Teodoro, A.C. (2018) Land Use / Land Cover ( LULC ) Using Landsat Data Series ( MSS , TM , ETM + and OLI ) in Azrou Forest , in the Central Middle Atlas of Morocco. *Environments*, 5, 1–16. doi:10.3390/environments5120131
- Priyono, P., Susilo, I., Karyono, K., Sigit, A.A. (2016) Analisis Profil Daerah Kabupaten Klaten Tahun 2002-2005. *Forum Geogr.*, 20, 27–46. doi:https://doi.org/10.23917/forgeo.v20i1.1802
- Richards, J. a, Jia, X. (2006) *Remote Sensing Digital Image Analysis, Methods*. doi:10.1007/3-540-29711-1
- Sari, N.M., Kushardono, D. (2014) Klasifikasi Penutup Lahan Berbasis Obyek Pada Data Foto Uav Untuk Mendukung Penyediaan Informasi Penginderaan Jauh Skala Rinci (Object Based Classification Of Land Cover On Uav Photo Data To Support The Provision Of Detailed-Scale Remote Sensing Informati. *Penginderaan Jauh*, 11, 114–127.
- Trisakti, B., Hamzah, R. (2013) Utilization of multi temporal sar data for forest mapping model development 10, 65–74. doi:http://dx.doi.org/10.30536/j.ijreses.2013.v10.a1844
- Tso, B., Mather, P.M. (2009) *Classification methods for remotely sensed data, Methods*. doi:10.4324/9780203303566
- Veci, L. (2015) *SENTINEL-1 Toolbox SAR Basics Tutorial*. Esa.

Zhang, M., Guo, H., Xie, X., Zhang, T., Ouyang, Z., Zhao, B. (2013) Identification of Land-Cover Characteristics Using MODIS Time Series Data : An Application in the Yangtze River Estuary 8. *Plos One* doi:10.1371/journal.pone.0070079.